

Learning Based Adaptive Force Control of Robotic Manipulation Based on Real-Time Object Stiffness Detection

Zhaoxing Deng, Xutian Deng and Miao Li

Abstract—Force control is essential for medical robots when touching and contacting the patient’s body. To increase the stability and efficiency in force control, an adaption module could be used to adjust the parameters for different contact situations. We propose an adaptive controller with an Adaption Module which can produce control parameters based on force feedback and real-time stiffness detection. We develop methods for learning the optimal policies by value iteration and using the data generated from those policies to train the Adaptive Module. We test this controller on different zones of a person’s arm. All the parameters used in practice are learned from data. The experiments show that the proposed adaptive controller can exert various target forces on different zones of the arm with fast convergence and good stability.

Index Terms—Force Control, Adaptive Control, Stiffness Detection, Value iteration.

I. INTRODUCTION

Contact is everywhere. To accurately control the exerted force when contacting with objects is crucial for medical robots and human-robot interaction. In a typical scenario of surgical applications, a robot can carry a medical device touching and scanning along a patient’s skin (Fig. 1), moving to the inspection position under the guidance of doctors, and incising tissues in the body. Force control plays a key role in those tasks. The robot should contact gently with different areas of the body and apply reference forces precisely. This requires the implemented controller to adjust to various contact environments and converge smoothly to the reference value.

Traditional force control methods include PI force control and impedance control. PI force control directly achieves target force through force feedback and PI control law [1]. It is simple and efficient, but it needs tuning the fixed parameters for each scenario. It also neglects the interaction between robots and environment; thus, it lacks robustness and may cause

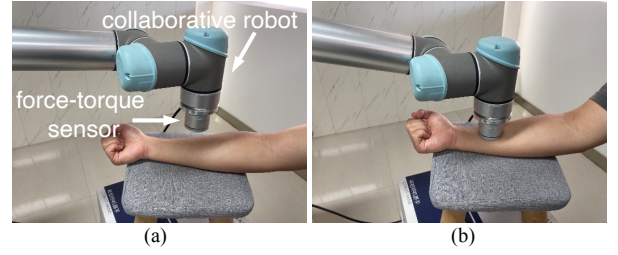


Fig. 1. A typical scenario for contact tasks. A robot is equipped with a force-torque sensor at the end-effector. (a) The robot end-effector is moving downwards. (b) The robot end-effector contacts a person’s arm with certain force.

instabilities and oscillations at contact. Impedance control indirectly control the interaction force between robots and environment through impedance control law [2]. It simulates interaction dynamics as a mass-spring-damper system and adjusts interaction forces and motions. It is suitable for applying a compliant behavior through contact, so it’s widely used in polishing[3], grasping[4] and coating tasks[5]. But lacks the ability to precisely track forces due to partial knowledge of the environment.

There are many adaptations of those classical methods. An adaptive controller based on stiffness detection and force feedback for grasping object task is proposed in [6]. It calculates the stiffness of the object and adjusts the force feedback gain with piecewise linear functions. However, it only focusses on grasping mental objects which have very small deformations. An impedance controller for force-tracking by adapting the control gains from estimated environment stiffness is described in [7]. The controller uses analytical solutions from LQR to calculate the control gains and EKF to estimate the environment stiffness. That method needs an accurate modelling of the robot dynamics as well as predefined parameters, thus lacks robustness for various types of environments.

One method to learn from the environment and improve the force adaptation is by using Dynamical Systems (DS) framework. In [8], an adaptive motion

Zhaoxing Deng is with Wuhan Cobot Technology Co., Ltd., Hubei, China, dengzhaoxing@cobotsys.com. Xutian Deng and Miao Li is with Department of Mechanical Engineering, Wuhan University, Hubei, China.

planning approach is used on impedance-controlled robots for polishing and pick-and-place tasks. Two types of parameterized time-independent dynamical systems (DS) are used for motion generation in different tasks. The parameters of the DS will be updated to adapt the robot's motion to human interactions. In [9], the time-independent DS-based control framework is extended to adjust both the trajectory and the force when performing contact tasks. The robot's nominal DS is used to generate the desired motion and contact force. In [10], a state-dependent force correction model is proposed to improve force tracking accuracy. Those methods need to learn the DS profile of the nonlinear surface.

Another method to enable robust physical interaction with the environment is to learn the constraints on the manipulated objects. In [11], a manifold learning approach is used to encode the Constrained Object Manipulations (COM) tasks. This achieves task-consistent adaptation based on an object-level impedance controller. The other method for motion and force adaptation is by using Reinforcement-Learning based controller. In [12] the Rapid Motor Adaptation algorithm (RMA) is proposed to allow legged robots move stably in difficult and changing terrains with changing payloads by real-time online adaptation. RMA has two subsystems: a base policy and an adaptation module. Those components are trained completely in simulation. The adaptation module is the key component of RMA which predicts the extrinsic vector using recent history of robot's states and actions. The trained controller can be deployed directly on the A1 robot without any fine-tuning.

DQN [13] and SAC [14] are two popular model-free learning methods in reinforcement learning. However, if we have a good model of the dynamics, we can adopt model-based learning such as value iteration [15] to effectively derive the optimal policy

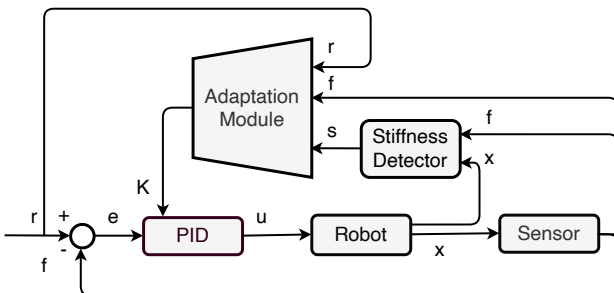


Fig. 2. The block diagram of the adaptive controller

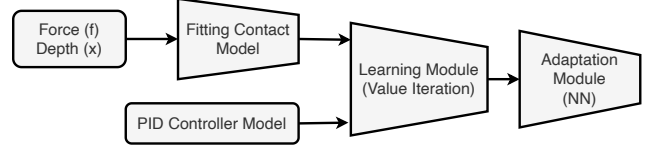


Fig. 3. The process for training the Adaptive Module

for discrete-time non-linear dynamic system.

To exploit the idea of learning from environment and training an adaptation module to improve versatility and stability, we propose an adaptive controller with an Adaptation Module which can adjust the parameters based on force feedback and real-time stiffness detection, as shown in Fig. 2. The Stiffness Detector computes the real-time stiffness of the object. The process for training the Adaptation Module is shown in Fig. 3. We first sample data from different zones of the environment and fit those data to model local dynamics of those zones. Then we build corresponding dynamic systems and use value iteration to learn the optimal policies for those dynamic models. Finally, we generalize the results to all parts of the environment by training a neural network to learn the relation between environment feature variables and controller parameters.

We present the design of the controller and training methods in section II. We evaluate the results of training processes and experiments on different zones of a person's arm in section III. We conclude with a discussion about the methods and future work in section IV.

II. METHODS

A. Designing the Adaptive Controller

The adaptive controller is based on a PID controller and an adaptive module which tunes the parameters for the PID controller. As seen from Fig. 2, the reference command r is fed into the system. The error $e = r - f$ is used as the input to the standard PID controller. The controller output u is then used to drive the robot towards the reference force

$$u = K_p e + K_i \int e dt + K_d \frac{de}{dt} \quad (1)$$

where K_p , K_i , K_d are parameters for the controller.

In a position-controlled robot, u can be the displacement within a control period. x is the position of the robot end-effector in Cartesian space. The force-torque sensor at the end-effector reads the current force value f and feeds that value to the Stiffness Detector as well as the Adaptation Module. The Stiffness

Detector uses the current force value and position to calculate the stiffness of the object. Notice stiffness here is defined as the slope of force-deformation curve and thus represents the local property of the material. The equation to calculate the real-time stiffness is

$$s = \frac{f_c - f_l}{dx_l} \quad (2)$$

where f_c is the current force value, f_l is the force value in last control period and dx_l is the displacement in last control period.

The output s is then passed to the Adaptation Module. The Adaptation Module uses the reference value r , the current force value f and current stiffness s to compute the adjustable parameters K for the PID controller.

B. Modeling Contact Dynamics from Data

We model the dynamic dynamics for using dynamical systems in model-based learning. We focus on the relationship between contact force and pressing depth (deformation) of a person's arm. We gather the data from some specific zones of the arm and generate approximation of dynamic model for other zones. From observation, when the pressing depth increases, the contact force as well as stiffness is also increasing smoothly. Thus, we can choose general exponential functions to fit the data

$$y = f(x) = a \exp(-bx) + c \quad (3)$$

where a , b , c are parameters in the exponential function.

We can use non-linear least squares to fit exponential functions to those curves.

C. Learning Optimal Policies using Value Iteration

Now that we obtain environment dynamic models and we know the output equation of the PID controller, we can design the dynamic systems as

$$\frac{dx}{dt} = K_p(f_r - f(x)) \quad (4)$$

where x is the state variable representing the depth of the deformation, K_p is the parameter in the PID controller, f_r is the reference value and f is the function of contact dynamics. Notice that for efficiency, we just include K_p as the parameter without K_i or K_d terms.

To learn the optimal policies given the dynamical systems and considering the discrete nature of real implementation of control program, we use value iteration algorithm. It's important that we choose K_p

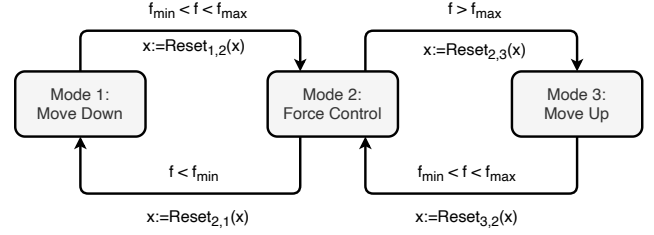


Fig. 4. The hybrid dynamical system for the control task

as the input to the system. The cost function is chosen to be in quadratic form

$$\min_{\pi(x)} \int_{t_0}^{\infty} [a(f_r - f(x))^2 + b(K_p)^2] dt \quad (5)$$

which pushes the system towards the equilibrium with a balance between speed and input magnitude.

D. Training the Adaptive Module from data

We learn the $K_p - x$ policies as the results from value iteration. Since each x relates to force f and its derivative $\frac{df}{dx}$ from the dynamic models, we can gather those discrete $K_p - x$ pairs and rewrite them to the corresponding $[K_p, f, \frac{df}{dx}]$ pairs. Here we assume that every area of the arm has similar dynamic property and $[f, \frac{df}{dx}]$ pair can fully capture that property at any pressing depth. Although we just sample data from some specific zones of the arm, we can generalize the learned policies to other areas of the arm given the feature $[f, \frac{df}{dx}]$. Since we treat reference value r as an independent environment variable and we learn the policies for various r , we also consider r as one input feature. Thus, our goal is to learn the function from input feature vector $[r, f, \frac{df}{dx}]$ to K_p .

Learning the approximate function from input features to output is a typical supervised learning problem. Consider the dimension of inputs and output as well as the amount of data, we choose a 3-layer fully connected neural network as the Adaptation Module architecture and train this neural network on input feature vectors and K_p .

E. Building a Hybrid Dynamical System

In practice, we build a hybrid dynamical system for the whole control task, as shown in Fig. 4. The control system consists of three modes:

- Mode 1: Moving downwards when contact force is smaller than the minimum gate f_{min} ;
- Mode 2: Using adaptive controller to exert the reference value;
- Mode 3: Moving upwards when contact force is larger than the maximum gate f_{max} .

The outputs will be reset when transiting from one mode to another mode.

III. EXPERIMENTAL EVALUATIONS

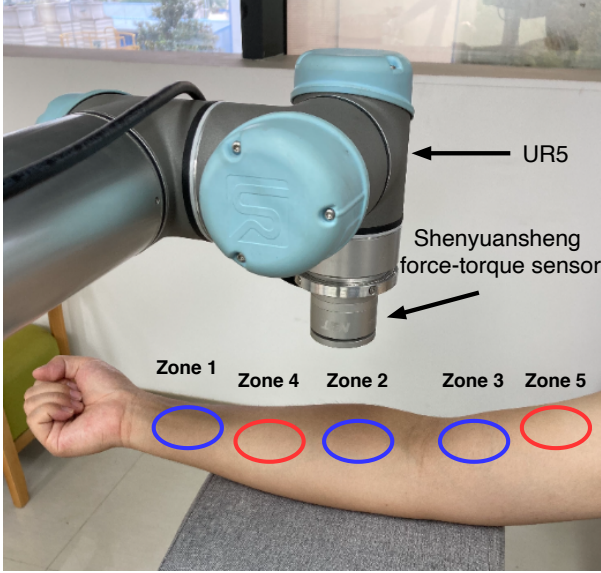


Fig. 5. Blue Zones are the areas to collect force depth data. Red Zones are two other areas on the arm..

In this section, we discuss the processes of training and experiment results. We evaluate our adaptive controller on a UR5 robot arm, as shown in Fig. 1. A Shenyuansheng force-torque sensor is attached to its end-effector. The control program is run on CobotSys 3.0 platform, which is an industrial robot operating system developed by Wuhan Cobot Technology Co., Ltd. The control loop rate for this program is 100Hz.

A. Fitting the Data for Dynamic Models

We collect data from three different Zones of a person's arm shown as the blue circles in Fig. 5. We programmed the robot end-effector to move straightly downwards at steady step size until the force being sensed reaches a certain amount. To compensate for the uncertainties in each experiment, we record 10 sets of data on each Zone and take their mean value. The relationships of force and depth at those three Zones are plotted as solid lines in Fig. 6.

Different Zones have different force-depth curves, but they all have similar shapes. Each curve is ascending smoothly with increasing slope. We fit those curves by exponential functions, which perfectly match the data (dashed lines in Fig.6).

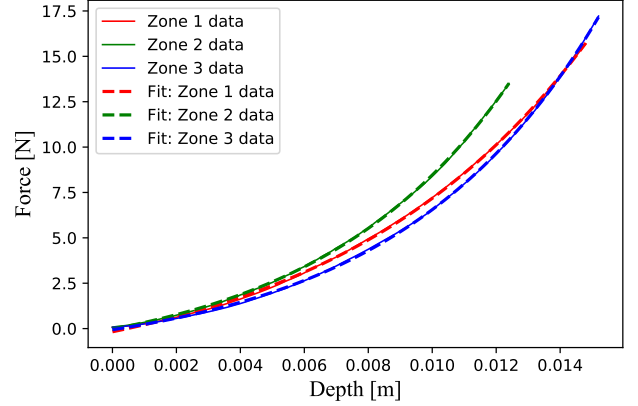


Fig. 6. The solid lines represent original data. The dashed lines represent the fitted functions.

B. Training the Adaptation Module

To build the dynamic systems and implement value iteration algorithm, we use Drake toolbox [16]. The state variable x is discretized to be between $[0, 0.02]$ with 1001 steps. The input variable K_p is discretized to be between $[0, 1]$ with 1000 steps. The parameters in cost function (5) are set to $a = 1$, $b = 40$. The time step is set to $0.03s$. We choose reference value r in the set $[4, 24]$ with step size 0.5. The optimal policies $K_p - x$ are computed for various values r from the three dynamic systems. Fig.7 shows $K_p - x$ policies for three Zones with r ranges from $5N$ to $20N$. It's easy to see that all $K_p - x$ functions have similar shapes. When r increases, the curves will be flatter, meaning K_p will starts smaller and moves slower along the x . Notice that when the reference value r is very small, there will be a little twist on the graph. That is the result of balancing between convergence rate and input magnitude and can be neglected. The results from value iteration are compatible with our intuition and suggest that the similar policy could be generalized to every other zone of the arm.

We build a 3-layer neural network for the Adaptation Module with layer sizes of $[6, 3, 1]$. The activation functions of all the nodes are ReLu functions. We train the Adaptation Module using supervised learning with input feature $[r, f, \frac{df}{dx}]$ and output label K_p . We use Adam optimizer to minimize MSE loss. We run the optimization process for 200 epoches with a learning rate of $1e-4$ and use a batch size of 64 split up into 4 mini-batches.

C. Testing on the arm

We test our adaptive controller on 5 Zones of the arm, as shown in Fig.5. The blue Zones represent

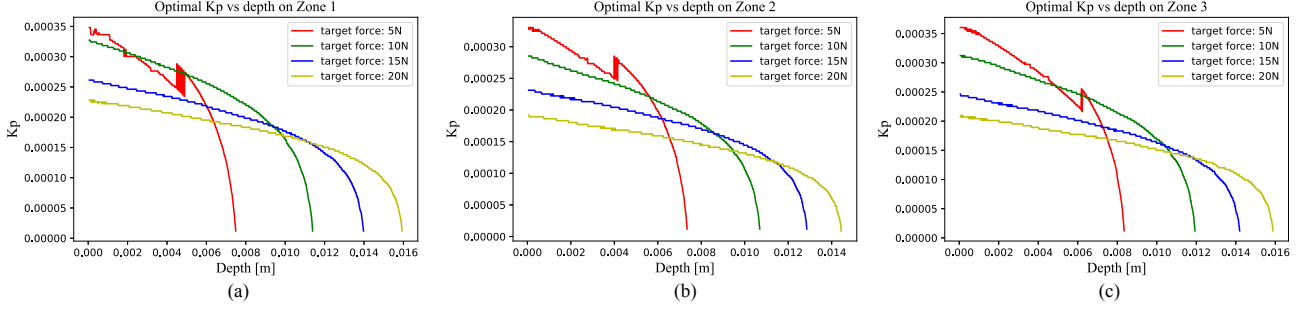


Fig. 7. The $K_p - x$ policies for each Zone at various reference values.

the places where we previously get the data for the dynamic models. The red Zones are other two areas on the arm. We range reference values from 5N to 20N. At the beginning of the experiments, the robot's end-effector will move straightly downwards, since it's in Mode 1 (Fig.8(a)). After it contacts the arm, it uses adaptive controller to exert reference force value on the arm.

Fig. 9 shows the experimental results for each Zone. The convergence time and overshoot will increase as the reference value increases. Typically the convergen time is within 1s. The overshoot is about 5N. Due to measurement noises from the force-torque sensor and disturbances of the arm (slight movement of the muscle), there will be some small variations after the curve converges. After all, the controller is very stable. The results show that our controller can converge to the reference value very soon. It can adapt to different contact zones of the arm with good stability and accuracy.

IV. CONCLUSION

In this paper, we propose an adaptive controller which has an Adaptation Module to adjust parameters for the underlying force controller. The Adaptive Module will take in the reference, current force value and real-time stiffness to output appropriate parameters. The real-time stiffness of the object is evaluated by the Stiffness Detector. We sample data from different zones of the environment and model the local dynamics for each zone. The optimal policies are learned by value iteration from dynamical systems. We then train the Adaptaion Module as a neural network to learn the relations between environment feature vectors and controller parameters. In this way we generalize the results to all zones of the environment. Finally, we build a hybrid dynamical system which combines the adaptive controller and other motion modes for the whole contact task. The experimental results show that our controller can adjust to various environments with good convergence rate, stability, and accuracy. The idea of Adaptation Module and learning from environment variables is a broad concept which can be extended to a general framework for adaptive controller design. In the future, we will replace the underlying force controller to admittance controller for better stability and consider encoding more environmental variables and constraints in the model to have better performance. We will focus on designing an adaptive controller for contact task on all parts the person's body.

ACKNOWLEDGMENT

The authors would like to acknowledge significant support from Wuhan Cobot Technology Co., Ltd and Wuhan University. The authors especially thank Professor Fei Chen for proofreading and suggestions. The authors also thank Dr. Dong Han and Chu Zhang for discussions about the main idea. In particular, the

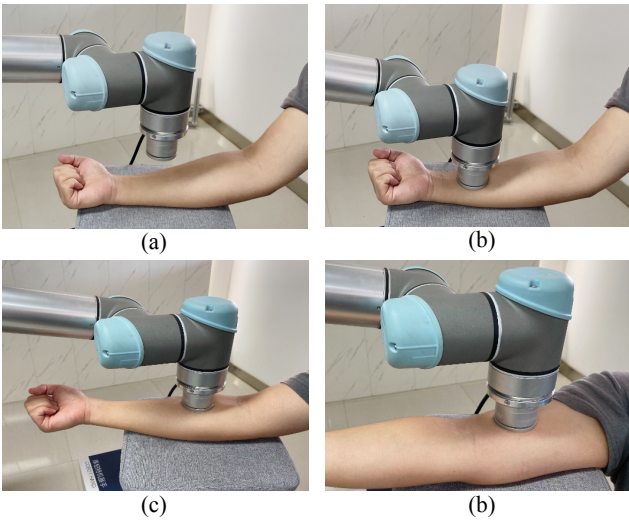


Fig. 8. Test the controller on different Zones of the arm. (a) The robot end-effector is moving straightly downwards. (b) (c) (d) show the end-effector contacts on different Zones.

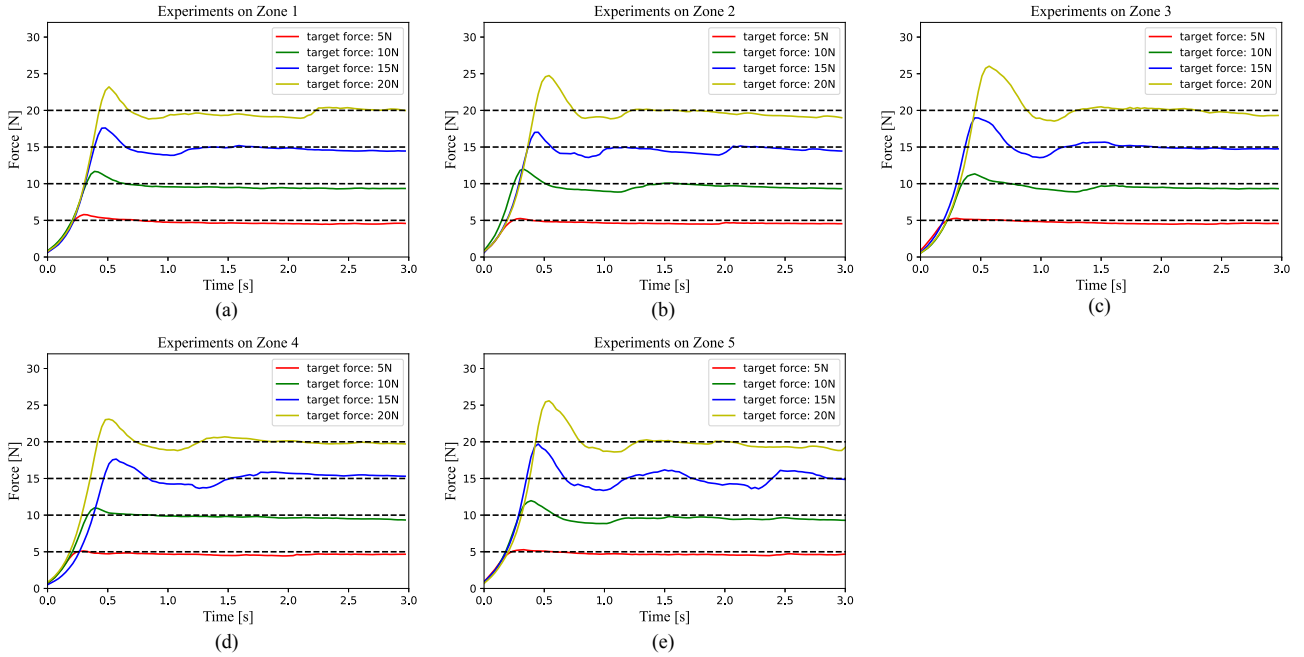


Fig. 9. The results of experiments for each Zone with various reference forces. (a) (b) (c) show the results on previously modeled areas. (c) (d) show results on other areas of the arm.

authors thank Yunchu Zhang for discussions on reinforcement learning techniques and Xiaofeng Chen for helping with the experiments.

REFERENCES

- [1] Kevin M. Lynch and Frank C. Park, *Modern Robotics: Mechanics, Planning, and Control*, 1st ed, Cambridge University Press, 2017, pp.436-439.
- [2] Neville Hogan, "Impedance control: An approach to manipulation," in *American Control Conference*, 1984, pages 304-313. IEEE, 1984.
- [3] A. M. Kabir, K. N. Kaipa, J. Marvel and S. K. Gupta, "Automated Planning for Robotic Cleaning Using Multiple Setups and Oscillatory Tool Motions," in *IEEE Transactions on Automation Science and Engineering*, vol. 14, no. 3, pp. 1364-1377, 2017.
- [4] Miao Li, Hang Yin, Kenji Tahara and Aude Billard, "Learning object-level impedance control for robust grasping and dexterous manipulation," 2014 *IEEE International Conference on Robotics and Automation (ICRA)*, pp. 6784-6791, 2014.
- [5] Yayun Du, Zhaoxing Deng, et al., "Vision and force based autonomous coating with rollers," 2020 *IEEE/RSJ International Conference on Intelligent Robots and Systems (IROS)*, pp. 9954-9960, 2020.
- [6] R. Andrecioli and E. D. Engeberg, "Grasped object stiffness detection for adaptive force control of a prosthetic hand," 2010 *3rd IEEE RAS-EMBS International Conference on Biomedical Robotics and Biomechatronics*, pp. 197-202, 2010.
- [7] Loris Roveda, Niccolò Iannacci, Federico Vicentini, Nicola Pedrocchi, Francesco Braghin, and Lorenzo Molinari Tosatti, "Optimal impedance force-tracking control design with impact formulation for interaction tasks," in *IEEE Robotics and Automation Letters*, 1(1):130-136, 2016.
- [8] M. Khoramshahi, A. Laurens, T. Triquet and A. Billard, "From Human Physical Interaction To Online Motion Adaptation Using Parameterized Dynamical Systems," 2018 *IEEE/RSJ International Conference on Intelligent Robots and Systems (IROS)*, pp. 1361-1366, 2018.
- [9] Walid Amanhoud, Mahdi Khoramshahi and Aude Billard, "A Dynamical System Approach to Motion and Force Generation in Contact Tasks", in *Robotics: Science and Systems (RSS)*, 2019.
- [10] W. Amanhoud, M. Khoramshahi, M. Bonnesoeur and A. Billard, "Force Adaptation in Contact Tasks with Dynamical Systems," 2020 *IEEE International Conference on Robotics and Automation (ICRA)*, pp. 6841-6847, 2020.
- [11] Miao Li, Kenji Tahara and Aude Billard, "Learning task manifolds for constrained object manipulation", *Autonomous Robots* 42, 159-174 (2018).
- [12] Ashish Kumar, Zipeng Fu, Deepak Pathak and Jitendra Malik, "RMA: Rapid Motor Adaptation for Legged Robots", in *Robotics: Science and Systems (RSS)*, 2021.
- [13] Volodymyr Mnih, Koray Kavukcuoglu, David Silver, et al., "Human-level control through deep reinforcement learning", *Nature* 518, 529-533 (2015).
- [14] Tuomas Haarnoja, Aurick Zhou, Pieter Abbeel and Sergey Levine, "Soft Actor-Critic: Off-Policy Maximum Entropy Deep Reinforcement Learning with a Stochastic Actor", in *Proceedings of the 35th International Conference on Machine Learning, PMLR* 80:1861-1870, 2018.
- [15] Russ Tedrake, *Underactuated Robotics: Algorithms for Walking, Running, Swimming, Flying, and Manipulation (Course Notes for MIT 6.832)*, 2021-6-14.
- [16] Russ Tedrake and the Drake Development Team, *Drake: Model-based design and verification for robotics*, 2019.